Indo. J. Chem. Sci. 14 (3) (2025)

Indonesian Journal of Chemical Science

http://journal.unnes.ac.id/sju/index.php/ijcs

Physiochemical Performance and Structural Characterization of Tobacco Stem Biochar under Various Pyrolysis Conditions for Sustainable Fertilizer Development

Mizanurafi' Ghifarhadi Prasiefa[1]✉, Daniyal Firmansyah[2]

[1]Department of Chemical Engineering, Faculty of Industrial Technology and Systems Engineering, Sepuluh Nopember Institute of Technology, Surabaya, Indonesia
[2]Department of Traditional Medicine, Vocational Faculty, Airlangga University, Surabaya, Indonesia

Article Info

Accepted : 10-07-2025

Approved : 01-10-2025

Published : 24-11-2025

Keywords:
Biomass Waste; Controlled Release Fertilizer; Pyrolysis; Tobacco Stem; Tobacco Stem Biochar; Sustainable Agriculture

Abstract

The development of Controlled Release Fertilizers (CRF) has emerged as a sustainable approach to minimize nutrient losses and mitigate environmental pollution caused by conventional fertilizers, which often result in 40–90% NPK loss. This study investigates the production and characterization of Tobacco Stem Biochar (TSB) through pyrolysis of tobacco stem powder under varying conditions to identify the most suitable material for CRF applications. Among the tested variants, TSB-3 which produced at 600℃ for 1 h with a heating rate of 30℃/min, demonstrated the most favorable properties. It exhibited a mass yield of 28.99%, fixed carbon content of 73.09%, porosity of 77.47%, surface area of 521.81 m²/g, and particle size of 555.68 µm. Chemical analysis revealed a pH of 9.51, nitrogen content of 24.18%, phosphorus 2.1%, potassium 1.8%, cation exchange capacity of 8.499 meq/100 g, electrical conductivity of 0.323 dS/m, and a salt index of 2.58. Enzymatic assays further confirmed promising biological activity, with 2.47 µmol/mL/min urease, 1.89 µmol/mL/min phosphatase, and 48.1 µmol/mL/min dehydrogenase. These results indicate that TSB-3 possesses the physicochemical and biochemical attributes required for nutrient retention and gradual release, making it a strong candidate for CRF formulation. Overall, this work highlights the potential of TSB to improve nutrient use efficiency, soil health, and sustainability in agricultural systems.

✉ Corresponding author:
E-mail: mizanurprasiefa@gmail.com; 6008222003@student.its.ac.id

p-ISSN 2252-6951
e-ISSN 2502-6844

Introduction

In the past two decades, the development of controlled-release fertilizers (CRF) has been actively pursued as a solution to nutrient inefficiency and environmental pollution caused by conventional fertilizers. Conventional fertilizers release nutrients rapidly, resulting in significant nutrient losses through volatilization, leaching, and surface runoff. According to Das and Ghosh (2022), up to 40–70% of nitrogen (N), 80–90% of phosphorus (P), and 50–70% of potassium (K) can be lost shortly after fertilizer application. These inefficiencies contribute not only to economic losses for farmers but also to serious environmental issues such as eutrophication, greenhouse gas emissions, and soil degradation. In response, CRF have emerged as an innovative alternative by controlling the nutrient release rate according to plant uptake needs, thereby improving fertilizer use efficiency (Y. Li, Yang, et al., 2025; Q. Wu et al., 2023).

Among the various types of CRF, biochar-based fertilizers (BBF) are considered a promising option due to their porous structure, environmental compatibility, and high carbon content (Lan et al., 2024; X.A. et al., 2020; Z. Z. Zhao et al., 2021). Biochar is a carbon-rich material produced through pyrolysis of biomass under limited oxygen conditions. It has gained widespread attention in recent years for its ability to improve soil fertility, enhance microbial activity, and serve as a carbon sequestration tool. Furthermore, biochar's porous structure can serve as a reservoir for nutrients, reducing nutrient leaching and enhancing controlled nutrient release (Liu et al., 2019; Ramesh et al., 2025). Tobacco stem (TS), a byproduct of the tobacco industry, is one potential biomass source that can be converted into biochar. In 2021, the Food and Agriculture Organization (FAO) reported that Indonesia was the fourth-largest tobacco-producing country globally, with a total production of 237,100 tons (Prasiefa & Zullaikah, 2025). According to Mulyatini et al. (2023), East Java was the highest contributor, producing up to 85,000 tons of tobacco in 2020. Despite the abundance of this agricultural waste, TS biomass is often left unused by farmers and burned in open fields, a practice that poses environmental risks due to the potential release of harmful compounds such as nicotine (Palupi et al., 2023).

Although biochar is widely recognized for its agronomic benefits, its low inherent nutrient content presents a major limitation for use as a CRF. Therefore, nutrient impregnation or nutrient loading techniques have been developed to improve the nutrient-holding capacity of biochar. limited exploration these materials can create synergistic effects Biochar is widely recognized for its agronomic benefits, such as improving soil structure, increasing water retention, and enhancing cation exchange capacity (CEC). For example, application of biochar has been reported to increase soil CEC by 20–50% and water-holding capacity by up to 15% depending on feedstock and pyrolysis conditions (Egamberdieva et al., 2022; Simmons, 2017; Wei et al., 2023). However, biochar typically contains low nutrient levels—for instance, less than 1–2% total nitrogen and <1% available phosphorus and potassium—which restricts its direct use in controlled release fertilizers (Lan et al., 2024; Prasiefa & Zullaikah, 2025). These limitations can be mitigated by selecting suitable biomass sources and optimizing pyrolysis parameters such as temperature, residence time, and heating rate. Previous studies show that increasing pyrolysis temperature from 400–600℃ can raise biochar surface area from ~50 m^2/g to over 500 m^2/g and porosity from below 40% to above 70%, while simultaneously reducing mass yield (Chowdhury et al., 2016; Dhar et al., 2022; Fernandes et al., 2020). Tobacco stem, with nitrogen content up to 2–3% and high lignocellulosic fractions, has demonstrated potential to produce biochar with favorable physicochemical characteristics for CRF applications under controlled pyrolysis (C. Li et al., 2022; Ramontja et al., 2025).

The interaction between pyrolysis temperature and biomass type may significantly affect the functional groups present on the surface of the biochar, which directly influence nutrient adsorption behavior and microbial interactions in the soil. For tobacco stem biomass specifically, compounds such as nicotine, alkaloids, and other organics may decompose differently at varied thermal regimes, potentially affecting both the safety and efficacy of the resulting biochar (Polat et al., 2016; H. Wang et al., 2018). Therefore, a comprehensive understanding of tobacco stem decomposition behavior under thermal treatment is essential.

Despite the promising potential of tobacco stem-derived biochar in agriculture, research evaluating the optimal production parameters of biochar from this specific biomass remains limited. Most studies either overlook the unique chemical composition of tobacco stem or fail to comprehensively evaluate its potential in controlled-release applications. Therefore, a more thorough investigation of the pyrolysis process using tobacco stem powder as feedstock is necessary to unlock its full potential as a CRF component.

This study is conducted to address these gaps by evaluating the influence of pyrolysis temperature and duration on the characteristics of biochar derived from tobacco stem powder. It is hypothesized that higher pyrolysis temperatures (up to 500℃) will enhance the fixed carbon (FC) content (>65%) and porosity (>60%) of the biochar, thereby improving its suitability for nutrient loading and controlled release applications. The main objective of this research is to identify the most efficient production methodology for Tobacco Stem Biochar (TSB) that meets the physical and chemical criteria for land remediation and agricultural use. The

results of this study are expected to contribute to the development of sustainable biochar-based fertilizers that utilize abundant agricultural waste and support environmentally friendly farming practices.

Methods

Materials and Instruments

The primary material used in this study was tobacco stem powder, which was locally sourced from tobacco farmers in East Java. The stems were cleaned, dried, and ground passed through a 60-mesh sieve. Distilled water (H_2O), obtained from the ITS Laboratory, was used in all experimental steps. Urea ($(NH_2)_2CO$), serving as an agricultural-grade nitrogen source. Analytical-grade chemicals—including sulfuric acid (H_2SO_4, 95–98%), potassium dichromate ($K_2Cr_2O_7$), glucose ($C_6H_{12}O_6$), selenium reagent (Se), boric acid (H_3BO_3), ethanol (C_2H_5OH, 96%), and methanol (CH_3OH, 99%)—were sourced from Merck. Other chemicals such as potassium chloride (KCl), ammonium acetate (CH_3COONH_4), sodium tungstate (Na_2WO_4), ammonium sulfate ($(NH_4)_2SO_4$), and sodium hydroxide (NaOH) were acquired from Merck and Sigma-Aldrich.

Buffer solutions were prepared in-house at the ITS Laboratory. These included phosphate buffer (pH 7), composed of H_3PO_4, $H_2PO_4^-$, and HPO_4^{2-}, and acetate buffers (pH 6.5 or 7.5) made using glacial acetic acid (CH_3COOH) and sodium acetate (CH_3COONa). Tris(hydroxymethyl)aminomethane (Tris, $(HOCH_2)_3CNH_2$), used in enzyme assays, was obtained from Sigma-Aldrich. Additional biochemical reagents included p-nitrophenyl phosphate (pNPP, $C_6H_4NO_3PO_4$), triphenyltetrazolium chloride (TTC, $C_{19}H_{15}ClN_4$), and triphenylformazan (TPF, $C_{19}H_{16}N_4$), with the latter synthesized in the ITS Laboratory. Nessler's reagent (K_2HgI_4) was used for the determination of ammonia content. Selenium reagents were also used to determine organic carbon content, and the Conway indicator was prepared in the laboratory. All reagents were of high purity to ensure accuracy in proximate analyses, water retention tests, and nutrient release studies. Additional information regarding reagent specifications can be found in the supplementary materials or provided upon request.

The equipment utilized in this study was essential for the preparation, characterization, and testing of TSB and controlled-release fertilizer formulations. A hammer mill was used to grind the tobacco stems into a fine powder, while a sieve shaker (B-ONE VTSS 200-9) was employed to separate particles by size. An analytical balance (OHAUS PX224/E) with a precision of 0.0001 g was used for accurate sample weighing. The pyrolysis process was conducted in a muffle furnace (Thermo Fisher Scientific THERMOLYNE FB1410M-33) with a capacity of 2.1 L, using a stainless-steel pyrolysis tube (TP 316L ASTM A269) to ensure durability and heat resistance. Orbital shakers (B-ONE COS-330D and Ruicheng TOS20) and a hot plate stirrer (B-ONE MHS-6) were used for solution mixing and sample homogenization. Moisture content (MC) was analyzed using an OHAUS MB95 moisture analyzer. Solution pH and conductivity were measured using a pH meter (OHAUS ST-300) and a conductivity meter (HORIBA LAQUA EC2000), respectively. Further material characterization was conducted using an X-ray diffractometer (XRD, PANalytical X'Pert PRO), an X-ray fluorescence spectrometer (XRF, PANalytical Prodigi), a surface area analyzer (Quantachrome NOVA 1200e), and a particle size analyzer (DSI Infitek PSA-LA2008A) to determine structure, composition, surface area, and particle distribution.

Pyrolysis Procedure of Tobacco Stem Biochar

The experimental procedure was divided into several key stages, beginning with the pyrolysis of tobacco stems into biochar. First, the tobacco stems were dried at 70℃ for 30 mins, then chopped and sieved to achieve a particle size of ≥50 mesh (≤0.297 mm) as shown in Fig. 1. The resulting powder was packed into a seamless stainless-steel pipe (16 cm in length, ¾" nominal diameter) with perforations to allow syngas escape and prevent pressure buildup during heating. The pipe was then placed in the muffle furnace and pyrolyzed at temperatures ranging from 500–700℃ for 1 to 4 hs as shown in Fig. 2. Following pyrolysis, the TSB was evaluated for yield, proximate and ultimate composition, CEC, Electrical Conductivity (EC), pH, and nutrient content (NPK), among other characteristics. Modifications to standard methods were made where appropriate and are detailed to ensure transparency and replicability of the methodology.

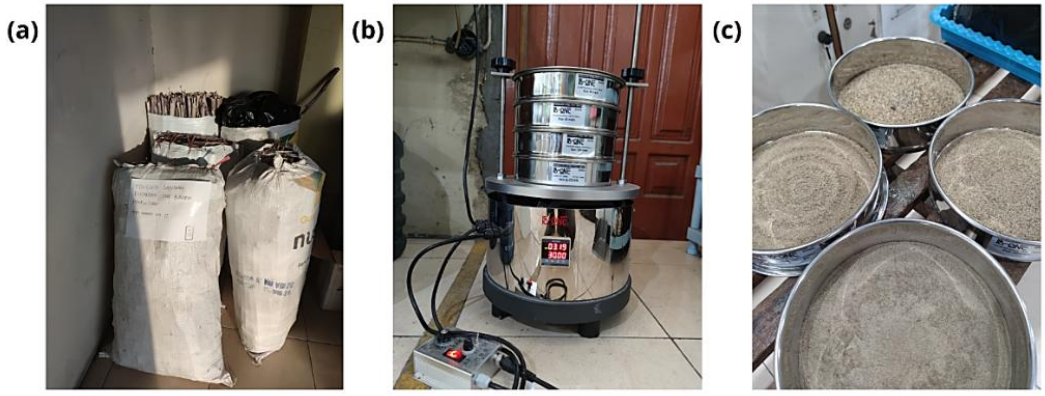

Fig. 1. Documentation of Tobacco Stem Powder Preparation; (a) Raw Tobacco Stem; (b) Sifted to ≥50 mesh (≤0.297 mm); (c) Resulting Tobacco Stem Powder

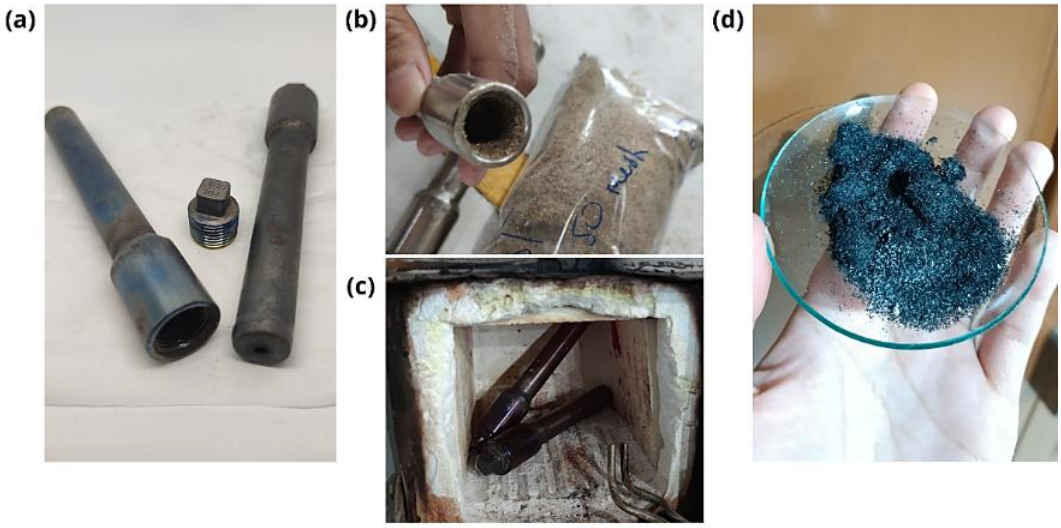

Fig. 2. Documentation of Pyrolysis of Tobacco Stem Powder into TSB (a) Pyrolysis Pipe; (b) Tobacco Stem Powder Inserted into the Pipe; (c) Pipe Inserted into the Furnace; (d) Resulting TSB (Biochar from Tobacco Stem)

Analytical Approaches for Evaluating Biochar Properties

The analysis of this research includes mass yield percentage, proximate (MC, volatile matter (VM), ash, FC, bulk density (BD), porosity, surface area using BET, pH value, ultimate (C, H, N, O), CEC, EC, and salt index (SI). Furthermore, the best TSB results will be analyzed enzyme activities (urease, phosphatase, dehydrogenase), XRF, XRD, SEM-EDX, particle size analysis (PSA). These comprehensive characterizations are intended to evaluate both the physicochemical and biological properties of the TSB and its potential application as a soil amendment and controlled-release fertilizer.

Mass yield of TSB is calculated as the percentage of TSB produced from the initial mass of the raw material, indicating the efficiency of the pyrolysis process. A higher mass yield suggests more efficient biomass conversion, which is essential for economic viability (Lin et al., 2016). Proximate analysis assesses MC, VM, ash content, and FC, following ASTM standards, providing insight into the combustibility and stability of the TSB. FC and ash content are especially critical in understanding thermal degradation behavior and nutrient retention (Racero-Galaraga et al., 2024).

BD, particle density (PD), and porosity are calculated to assess the physical structure of the samples (Blake, 2015; Blake & Hartge, 2018; Flint & Flint, 2018). BET analysis measures the specific surface area of TSB, which correlates with adsorption capacity, while PSA evaluates particle size distribution, influencing soil texture compatibility (Gee & Or, 2018; Y. Wang et al., 2023).

Ultimate analysis focuses on the content of C, H, N, and O in the samples, with oxygen calculated as the remainder after measuring the other elements. These parameters influence the reactivity, hydrophilicity, and decomposition rate of the TSB. Nutrient content (NPK) is analyzed using atomic absorption spectroscopy. Water absorption capacity is also measured to evaluate the potential of TSB to retain MC in

the soil, an important trait under water-scarce conditions (Y. Li, Sang, et al., 2025; Mohd Fairulnizal et al., 2019; Siewruk & Szulc, 2023; Yi et al., 2017).

pH values for tobacco powder and TSB are determined by using established protocols, as pH affects microbial dynamics and nutrient solubility (Shahid et al., 2023). CEC is determined to estimate nutrient availability in the substrate, while EC and SI evaluate the ionic concentration and salinity stress risk in the samples (Chapman, 2016; X. Li et al., 2016). Enzyme activities of urease, phosphatase, and dehydrogenase are measured to assess microbial activity and nutrient cycling, which are critical for soil fertility and plant health (Attademo et al., 2021).

XRF and XRD analyses are conducted to identify mineral compositions and crystal structures, useful for tracking the stability and transformation of mineral phases during pyrolysis. SEM-EDX provide morphological and elemental information on the surface (Fatimah et al., 2022; Schulz et al., 2020; Y. Y. Wang et al., 2020). All methods are performed in duplicates to ensure accuracy and reproducibility.

Results and Discussion

The pyrolysis process begins at ambient temperature (27–30℃) with an overall heating rate of 30℃/min. The heating rate accelerates between 50℃ and 450℃, reaching an average of 37.39℃/min due to the rapid thermal decomposition of the main organic components of biomass: hemicellulose, cellulose, and lignin. Hemicellulose decomposes within the range of 130–260℃, cellulose between 240–360℃, and lignin from 280–500℃ (Mohan et al., 2015). These stages contribute to the release of volatile compounds and the transformation of the tobacco stem matrix into a carbon-rich structure. As the temperature continues to rise between 570℃–700℃, the heating rate decreases to 14.22℃/min, indicating the near-complete decomposition of organic constituents and the formation of stable carbonaceous residues (Weber & Quicker, 2018).

The TSB obtained from this process exhibits varying physical and chemical properties depending on the specific pyrolysis conditions, including temperature and duration. The complete data for all TSB samples, including yield, pH, EC, proximate analysis, and elemental composition, are summarized in Table 1, along with their corresponding operational conditions.

Table 1. Characterization of Tobacco Stem Biochar (TSB)

Parameters	Variety of Tobacco Stem Biochar (TSB)						
	1	2	3	4	5	6	7
Pyrolysis Temperature (℃)	500	550	600	650	700	700	600
Pyrolysis Time (h)	1	1	1	1	1	2	4
Mass Yield (%)	29.28	2.,22	28.99	26.71	26.27	29.07	27.22
Moisture Content (%)	7.86	7.48	4.16	3.20	2.79	2.37	3.00
Volatile Matter (%)	15.44	13.62	2.07	3.75	4.35	4.94	4.06
Ash (%)	20.36	20.43	20.68	21.81	22.20	35.82	23.73
Fixed Carbon (%)	56.34	60.29	73.09	71.24	70.65	56.87	69.21
Bulk Density (g/mL)	0.15	0.14	0.12	0.14	0.14	0.16	0.15
Porosity (%)	72.29	73.18	77.47	75.43	74.32	71.01	71.91
BET Surface Area (m²/g)	428.33	470.18	521.81	502.48	491.81	443.63	471.64
Particle Size (micron)	-	-	555.68	-	-	-	-
Particle Size (mm)	-	-	0.56	-	-	-	-
Particle Size (mesh)	-	-	26.81	-	-	-	-
pH Value	9.29	9.37	9.51	9.70	9.91	10.19	9.97
Carbon Content (%)	33.29	36.69	51.04	48.27	45.38	34.43	41.43
Hydrogen Content (%)	0.29	0.30	0.34	0.39	0.42	0.31	0.37
Nitrogen Content (%)	27.74	26.69	24.18	24.88	25.39	25.58	25.09
Oxygen Content (%)	14.28	12.12	3.76	4.65	6.61	3.86	9.38

Parameters	Variety of Tobacco Stem Biochar (TSB)						
	1	2	3	4	5	6	7
Cation Exchange Capacity (meq/100g)	11.00	12.50	8.49	9.50	12.99	14.99	13.99
Electrical Conductivity (dS/m)	0.45	0.53	0.32	0.41	0.68	1.11	1.09
Salt Index	3.58	4.22	2.58	3.24	5.43	8.91	8.74
Phosphorus Content (%)	-	-	2.10	-	-	-	-
Potassium Content (%)	-	-	1.80	-	-	-	-
Urease (µmol/mL/min)	-	-	2.47	-	-	-	-
Phosphatase (µmol/mL/min)	-	-	1.89	-	-	-	-
Dehydrogenase (µmol/mL/min)	-	-	48.10	-	-	-	-

The highest mass yield was observed in TSB-6 at 29.07%, while the lowest yield was recorded in TSB-5 at 26.27%. Overall, despite variations in pyrolysis temperature and duration, the mass yield remained relatively stable, ranging from 26.71% to 29.28%. This consistency indicates that the process was well-controlled, and that the thermal degradation of biomass reached a plateau across the tested conditions.

Physiochemical Properties

Proximate analysis was conducted to identify MC, VM, ash, and FC in both raw TS powder and the resulting TSB. This analysis was performed to demonstrate that the pyrolysis process successfully increased the FC content while simultaneously reducing MC and VM. As shown in Fig. 3, pyrolysis specifically reduced MC and VM, while increasing ash and FC contents. This confirms that the thermal decomposition process effectively reduces MC and VM (Sukamto et al., 2016; X. Yang et al., 2018). The MC content in the raw TS powder was initially 9.96%, which then decreased significantly in the following order: TSB-1 > TSB-2 > TSB-3 > TSB-4 > TSB-7 > TSB-5 > TSB-6, with the lowest MC observed in TSB-6 at 2.37%. The overall trend shows that MC decreases with increasing pyrolysis temperature and duration. Similarly, VM content also decreased drastically in the following order: TSB-1 > TSB-2 > TSB-6 > TSB-5 > TSB-7 > TSB-4 > TSB-3, with the lowest VM recorded in TSB-3 at 2.07%, compared to 68.47% in raw TS powder. An increase in pyrolysis temperature from 500–600℃ for 1 h resulted in a further reduction of VM. However, when the pyrolysis temperature was raised to 650℃ or the duration was extended to 4 h, the VM content increased instead. This phenomenon can be attributed to partial recondensation, wherein volatilized compounds recondense and become trapped within the pores of the TSB matrix, thereby increasing the VM content despite the majority having already been released (Zhu et al., 2023).had the highest ash content (35.82%)

The ash content increased progressively with higher pyrolysis temperatures and longer residence times, following the order TSB-1 > TSB-2 > TSB-3 > TSB-4 > TSB-5 > TSB-6 > TSB-7, with the highest value observed in TSB-6 (35.82%), compared to only 2.38% in raw TS powder (Fig. 3). The substantial increase in ash content in TSB-6 at 700℃ for 2 h indicates that the optimal condition had been exceeded, leading to excessive degradation of the carbon structure (Braga et al., 2022). The final proximate parameter, FC, represents the residual fraction of TSB after deducting MC, VM, and ash. The FC content increased significantly compared to raw TS powder, which contained only 19.2%. The order of FC was TSB-3 > TSB-4 > TSB-5 > TSB-7 > TSB-2 > TSB-6 > TSB-1, with the highest value recorded in TSB-3 (600℃, 1 h) at 73.09% (Fig. 3). These results suggest that TSB-3 represents the most favorable condition for the pyrolysis of TS powder.

The proximate analysis results demonstrated that the pyrolysis process effectively altered the characteristics of TS powder by increasing FC while reducing MC and VM. Pyrolysis conditions, specifically temperature and residence time, had a significant influence on the properties of the resulting TSB. However, excessively high temperatures and prolonged residence times led to higher ash content due to continuous degradation and increased VM content due to partial recondensation (C. Wang et al., 2019). As a comparative benchmark, the quality standards for biochar as fertilizer are provided by the European Biochar Certificate and SNI 19-1730-2004 as shown in last row of Table 2. When MC is too high (≥15%), it decreases carbon storage efficiency and adsorption capacity; if VM exceeds the threshold (≥40%), it can cause phytotoxic effects (compounds that may lead to cell death or inhibit plant growth); when ash content is above the standard (≥50%), it may increase heavy metal contamination and excessively elevate soil pH; while FC below the standard (≤50%) reduces carbon stability in soil and decreases porosity (An et al., 2021; Chen et al., 2021; Helepciuc Gradinaru et al., 2017). Based on these comparative standards, TSB-3 produced

in this study is considered suitable for application as a soil amendment. The comparative trends of MC, VM, ash, and FC between TS powder and TSB are illustrated in Fig. 3.

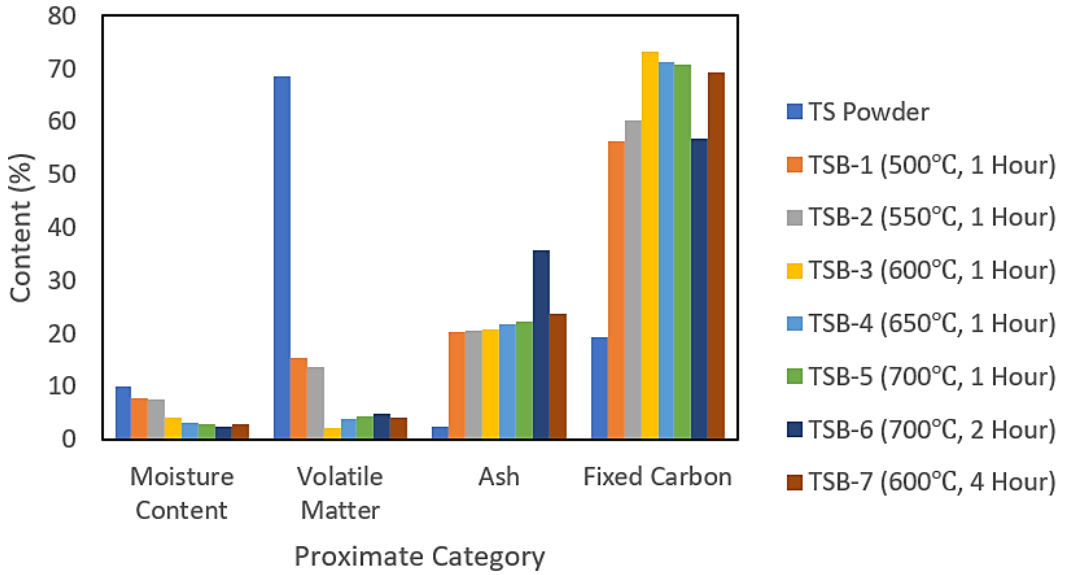

Fig. 3. Comparison Graph of Proximate Test Results os TS Powder and TSB

The porosity test was conducted by calculating BD and PD. BD refers to the mass of material per total volume, including the void spaces between particles, while PD represents the mass of material per unit volume of the particles themselves, excluding inter-particle voids. Porosity reflects the proportion of empty spaces within a material, indicating the capacity to retain water, nutrients, and microorganisms. Lower BD values correspond to higher porosity percentages (Flint & Flint, 2018; Prasiefa & Zullaikah, 2025).

Pyrolysis effectively reduced BD while increasing porosity. This finding confirms that thermal decomposition enhances inter-particle pore structures (S. X. Zhao et al., 2017). The BD of the raw BT powder was initially 0.181 g/mL, which decreased after pyrolysis in the sequence TSB-6 > TSB-1 > TSB-7 > TSB-5 > TSB-4 > TSB-2 > TSB-3, with the lowest BD recorded in TSB-3 at 0.116 g/mL. In contrast, PD values did not show significant variation among the TSB samples, suggesting that changes occurred mainly in pore spaces rather than within the internal material density (Sorrenti et al., 2016). The porosity of raw biomass was 65.96%, which increased most significantly in TSB-3 to 77.47%, followed by TSB-4 > TSB-5 > TSB-2 > TSB-1 > TSB-7 > TSB-6.

In general, higher pyrolysis temperature and longer residence time are expected to decrease BD and increase porosity (Qurat-ul-Ain et al., 2021). However, the present findings deviate from this trend: while increasing the temperature from 500–600℃ enhanced porosity, a further increase to 650℃ resulted in a decline. This phenomenon can be explained by the proximate analysis results. TSB-6 (ash 35.82%; FC 56.87%) exhibited the lowest porosity (71.01%) due to excessive ash, which filled available pores and increased density (Zheng et al., 2019). Conversely, TSB-3 (ash 20.68%; FC 73.09%) demonstrated the best performance, as higher FC contributed to a more porous structure (Rahmat et al., 2025). This porosity test further supports that TSB-3 (600℃, 1 h) represents the optimal pyrolysis condition in this study as shown in Fig. 4.

European Biochar Certificate (EBC) and SNI 19-1730-2004,

For comparison, the last row of Table 2 presents reference values for high-quality biochar intended for fertilizer application (Blanco-Canqui, 2017; Melo et al., 2022). If BD is too low (<0.1 g/mL), biochar becomes difficult to apply to soil due to its lightweight nature, making it easily dispersed by wind or water. Conversely, excessively high BD (>0.6 g/mL) results in compact biochar that reduces water and nutrient retention capacity (Birol & Günal, 2025). Similarly, biochar with too low porosity (<60%) is ineffective for storing water and nutrients, whereas overly high porosity (>90%) makes the material fragile and prone to degradation (D. Wang et al., 2019). Based on these comparative standards, TSB-3 is suitable for use as a soil amendment.

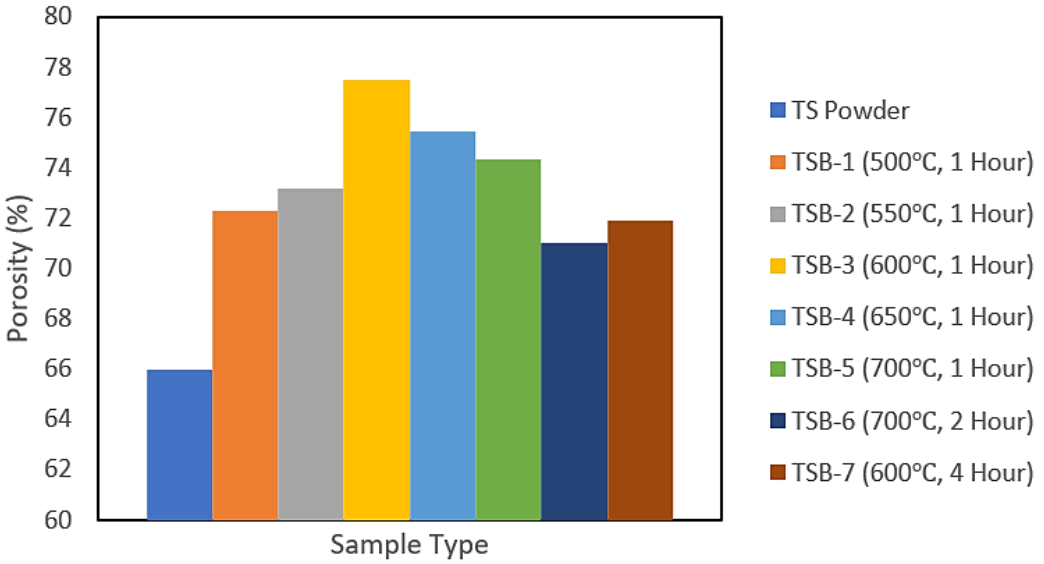

Fig. 4. Comparison Graph of Porosity Analysis Results os TS Powder and TSB

Table 2. Proximate Composition, Density, and Porosity of Biochar Samples at Various Pyrolysis Conditions

Sample Type	Proximate Category (%)				Density & Porosity		
	Moisture Content	Volatile Matter	Ash	Fixed Carbon	Bulk Density (g/mL)	Particle Density (g/mL)	Porosity (%)
TS Powder	9.96	68.47	2.38	19.20	0.18	0.53	65.96
TSB-1	7.86	15.44	20.36	56.34	0.15	0.55	72.29
TSB-2	7.48	13.62	20.43	60.29	0.14	0.50	73.18
TSB-3	4.16	2.07	20.68	73.09	0.12	0.52	77.47
TSB-4	3.20	3.75	21.81	71.24	0.14	0.57	75.43
TSB-5	2.79	4.35	22.20	70.65	0.14	0.56	74.32
TSB-6	2.37	4.94	35.82	56.87	0.16	0.56	71.01
TSB-7	3.00	4.06	23.73	69.21	0.15	0.52	71.91
Standard	≥15%	≥40%	≥50%	50%	>0.1 g/mL	-	>60%

After completing the proximate and porosity analyses, the surface area of TSB was evaluated to determine the effectiveness of the material in adsorbing and retaining nutrients and water, both of which are essential for plant growth. As shown in Fig. 5, TSB-3 exhibited the highest surface area of 521.81 m²/g, followed by TSB-4 > TSB-5 > TSB-7 > TSB-2 > TSB-6 > TSB-1. The trend indicates that increasing pyrolysis temperature from 500–600°C enhanced the surface area, but a further increase in temperature led to a decline, as excessively high temperatures can damage the carbon structure. This result correlates with the proximate analysis discussed previously: higher FC content tends to increase surface area, whereas higher VM and ash contents reduce it. For instance, TSB-3 (VM 2.07%; ash 20.68%; FC 73.09%) achieved a surface area of 521.81 m²/g, while TSB-1 (VM 15.44%; ash 20.36%; FC 56.34%) showed only 428.33 m²/g. These findings confirm that TSB-3 (600°C, 1 h) represents the optimal condition for producing biochar suitable for agricultural applications. For comparison, previous studies reported that biochars with surface areas exceeding 40 m²/g are already considered to be of good quality for agronomic use (Das & Ghosh, 2022; Xu et al., 2025). Fig. 5 presents the comparative results of surface area across different pyrolysis temperatures and residence times.

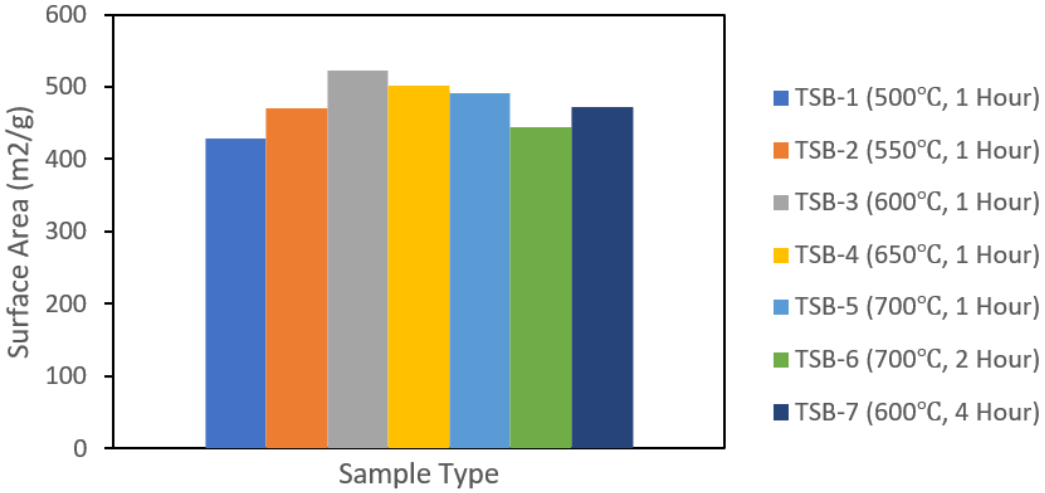

Fig. 5. Graph of Surface Area Analysis Results of TSB

Chemical Characteristics

In general, biochar exhibits amphoteric properties, meaning it can act as either an acid or a base depending on environmental conditions. Typically, the pH of biochar increases compared to its raw biomass feedstock, which is attributed to lignocellulose decomposition and the formation of functional groups. Carboxyl groups (-COOH) are generated through partial oxidation during pyrolysis, while hydroxyl groups (-OH) are produced through incomplete dehydration and condensation reactions. The presence of these groups contributes to the alkalinity of biochar surfaces, particularly when dissociation occurs in aqueous solution (Huang et al., 2019; Shi et al., 2017). Upon dissociation, -COOH and -OH groups release H^+ ions, forming anions ($-COO^-$ and $-O^-$) that behave as bases. These anions subsequently attract protons from water, generating hydroxide ions (OH^-) in solution and thus increasing alkalinity (Fang et al., 2018; John et al., 2014). The pH of the initial BT powder was measured at 6.52 and increased significantly after pyrolysis. This phenomenon correlates with the ash content in the TSB, as alkaline minerals in ash (e.g., K, Ca, Mg) interact with functional groups to form basic salts when dissolved. Consequently, the pH of TSB-1 (ash 20.36%) reached 9.29, while TSB-6 (ash 35.82%) showed a higher pH of 10.19.

The decrease in C content observed in TSB-4 to TSB-7 during ultimate analysis is primarily attributed to excessive carbonization, which occurs as both pyrolysis temperature and residence time increase (X. F. Wu et al., 2019; Yashim et al., 2016). O and N contents also declined as the pyrolysis temperature rose from 500–600℃, correlating with the reduction in VM observed in proximate analysis. However, both elements increased again when the temperature was elevated to 650℃ or when the residence time was extended to 4 h. This rebound is likely due to recondensation processes occurring at higher thermal conditions as shown in Table 1 (Cui et al., 2020; Jiang et al., 2021; T. Yang et al., 2023).

CEC testing demonstrates the ability of a material to exchange cations with its medium. The CEC value serves as an indicator to measure the sample's capacity to retain cations available for plant growth and release them in a controlled manner (Ćirić et al., 2023). EC and SI analyses were carried out to further evaluate the quality of TSB as a potential soil amendment and fertilizer component by assessing the concentration of soluble salts (dos Santos et al., 2021). These parameters are essential to ensure that the material does not exhibit phytotoxicity at elevated concentrations.

The percentage of ash and FC from proximate analysis strongly influences the values of CEC, EC, and SI of TSB. Higher ash content generally increases EC, since ash contains various inorganic minerals capable of releasing ions when dissolved in water (Fahmi et al., 2019; Wardman et al., 2012; Zulkifli et al., 2021). In contrast, higher FC leads to lower EC values, as its inert and stable nature does not contribute significantly to the release of soluble ions (Arbuzov et al., 2024; Shin, 2015). This explains why the EC of TSB-3 (ash 20.68%; FC 73.09%) was only 0.323 dS/m, while that of TSB-6 (ash 35.82%; FC 56.87%) reached 1.114 dS/m. Moreover, EC values in this study were broadly proportional to CEC, because minerals in ash provide ion-exchange sites that enhance CEC, whereas a high proportion of stable FC lacks active functional groups, thereby reducing CEC (Greinert et al., 2019; Weisenberger et al., 2020).

pH ranged from 8.34 to 10.59, with TSB-6 being the most alkaline; extreme alkalinity may disrupt soil microbes. TSB-3 also had the highest CEC (74.83 $cmol^+/kg$)

The CEC of 5–40 meq/100 g is considered an indicator of good quality growth media (Oktariani et al., 2023; Suwardi et al., 2023), and this standard can also be applied to materials intended for fertilizer use. If the CEC value is too low (<5 meq/100 g), plants may suffer from nutrient deficiency because essential nutrient ions cannot be retained for long periods and are easily leached by water. Conversely, if the CEC value is too high (>40 meq/100 g), nutrient deficiency may also occur since too many ions are tightly bound to the material and thus unavailable for plant uptake (E. & V., 2023; M. Yang et al., 2024). The acceptable EC threshold is <2 dS/m for growth media and <3 dS/m for fertilizer, while SI values <50 are generally considered safe for plants. Excessively high EC may impair water absorption and cause salt toxicity due to salinity effects, whereas excessively low EC may result in insufficient nutrient ion availability (Chrysargyris & Xylia, 2021; Vyavahare et al., 2023). The results indicated that TSB-3 complied with these safety limits, confirming its suitability for agricultural applications. In terms of pH, values within the range of 6–10 are favorable for plant growth environments. A pH above 10 may inhibit the uptake of essential micronutrients, while excessively low values (<6) may increase the solubility of heavy metals, posing potential risks to plants (Fidel et al., 2018; Xue et al., 2016).

TSB-3 (600℃, 1 h)

It recorded the highest fixed carbon (73.09%), porosity (77.47%), and surface area (521.81 m^2/g), while achieving the lowest volatile matter (2.07%) and bulk density (0.116 g/mL).
(69.13%)

Structural and Elemental Analysis

XRF, XRD, and SEM-EDX analyses of TSB-3 confirm the presence of essential nutrients such as potassium (K), phosphorus (P), calcium (Ca), magnesium (Mg), and silicon (Si). These elements are vital for plant growth and soil health. XRD patterns show a transition from semi-amorphous to crystalline structures, indicating the successful deposition and structural organization of mineral phases during pyrolysis and impregnation processes. Crystalline peaks observed for compounds like $CaCO_3$, KCl, and SiO_2 reflect the enhanced mineral stability and slow-release characteristics desirable in agricultural applications (Alcazar-Ruiz et al., 2021; Alderton, 2020).

Fig. 6 shows the results of XRF and XRD analysis on TSB-3, highlighting the prominent elemental and mineralogical compositions. Meanwhile, SEM analysis on TSB-3 at various magnifications as shown in Fig. 7, illustrates the highly porous surface morphology, increased surface roughness, and heterogeneity—all of which facilitate nutrient adsorption and microbial colonization (Nan et al., 2023; Zarzuela et al., 2023). The results obtained for TSB indicate the TSB's suitability for agricultural and environmental applications.

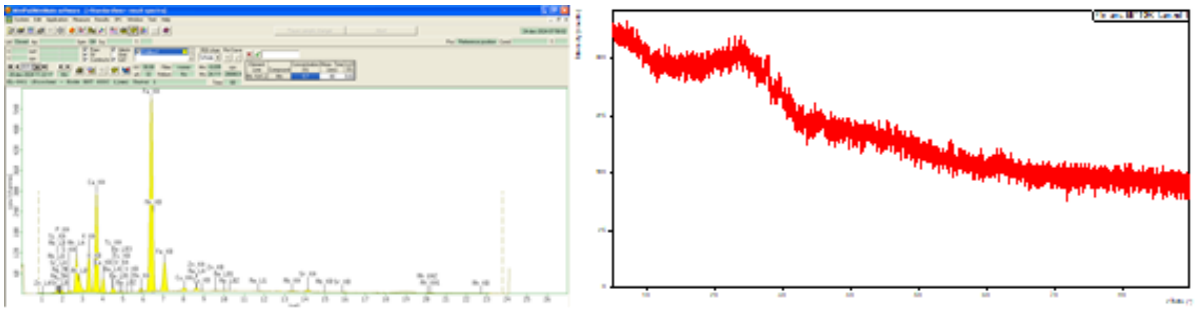

(a) **(b)**

Fig. 6. (a) XRF Analysis Result of TSB-3; (b) XRD Analysis Result of TSB-3

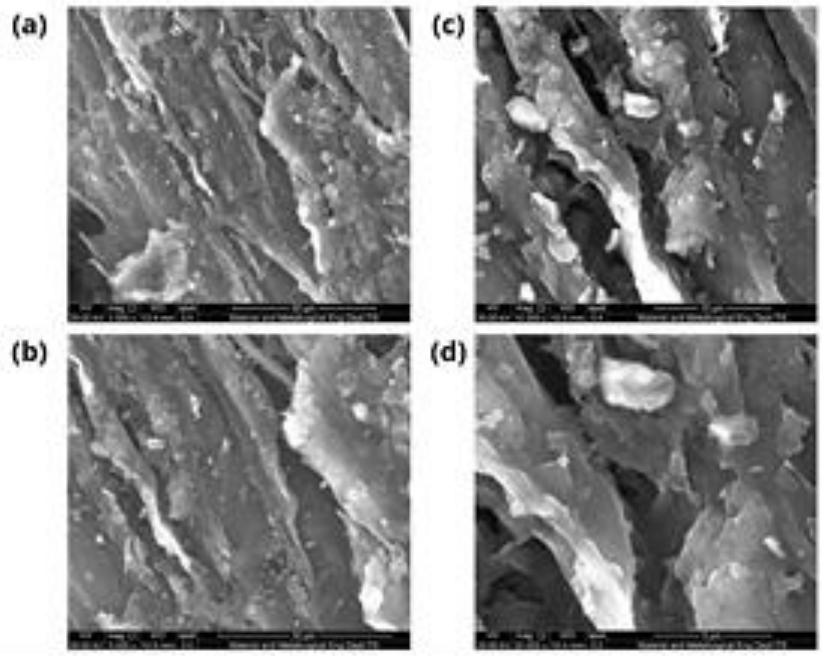

Fig. 7. SEM Analysis Result of TSB-3 Magnification (a) 2500×; (b) 5000×; (c) 10000×; (d) 20000×

Particle size analysis shows that pyrolysis significantly reduces particle size, enhancing environmental interaction efficiency. TSB-3 has an average particle size of 555.68 μm. Surface area analysis via BET indicates TSB-3 has the high surface area and porosity, making it suitable for nutrient retention. The TSB results are considered better or at least comparable to those reported in previous studies. A high surface area, particle size distribution, and porosity are crucial for improving the sorption of nutrients and water retention in soil, especially under drought-prone or nutrient-deficient conditions. These characteristics not only enhance the physical structure of the soil but also create more favorable habitats for microbial colonization, further promoting soil fertility (Fidel et al., 2018; Xue et al., 2016).

TSB shows performance that matches or surpasses that of earlier studies. However, for the TSB parameters that remain outside the standard range or differ from previous studies, further improvement is necessary. Therefore, subsequent research should focus on impregnating the biochar with nutrient solutions or compositing it with hydrogel to meet the required standards and align more closely with the findings of earlier studies. Such enhancements could increase the efficiency of nutrient release and retention, improve soil health, and contribute to the development of sustainable, high-performance biochar-based fertilizers.

Conclusion

This study confirmed that pyrolysis of tobacco stem powder produces biochar with suitable properties for agricultural use. Among the tested conditions, TSB-3 (600℃, 1 h) showed the best performance, with the highest FC, porosity, and surface area, indicating strong stability and nutrient retention capacity. The physicochemical analysis (XRF, XRD, SEM-EDX) further revealed that TSB-3 contained essential nutrients, stable mineral structures, and favorable cation exchange capacity. These characteristics demonstrate its potential as a soil amendment and as a component in controlled-release fertilizer. Overall, TSB can improve soil fertility, water management, and contribute to sustainable agriculture.

Acknowledgments

The authors gratefully acknowledge the financial support from Program Riset Inovatif Produktif – Indonesia–NTU Singapore Institute of Research for Sustainability and Innovation (RISPRO–INSPIRASI, No. 6637/E3/KL.02.02/2023) and Universitas Gadjah Mada (No. 13577/UN1.P/DPU/HK.08.00/2023). We would also like to thank the laboratory staff at the Department of Chemical Engineering, Institut Teknologi Sepuluh Nopember (ITS), for their assistance during the experimental work. Their technical guidance and provision of essential facilities greatly contributed to the smooth execution of this research. This research would not have been possible without the collective efforts of all individuals and institutions involved.

References

Alcazar-Ruiz, A., Ortiz, M. L., Sanchez-Silva, L., & Dorado, F. (2021). Catalytic effect of alkali and alkaline earth metals on fast pyrolysis pre-treatment of agricultural waste. *Biofuels, Bioproducts and Biorefining*, *15*(5), 1473–1484. https://doi.org/10.1002/bbb.2253

Alderton, D. (2020). X-Ray Diffraction (XRD). In *Encyclopedia of Geology: Volume 1-6, Second Edition* (Vol. 1, pp. 520–531). Elsevier. https://doi.org/10.1016/B978-0-08-102908-4.00178-8

An, Z., Bernard, G. M., Ma, Z., Plante, A. F., Michaelis, V. K., Bork, E. W., Carlyle, C. N., Baah-Acheamfour, M., & Chang, S. X. (2021). Forest land-use increases soil organic carbon quality but not its structural or thermal stability in a hedgerow system. *Agriculture, Ecosystems and Environment*, *321*. https://doi.org/10.1016/j.agee.2021.107617

Arbuzov, A. B., Muromtsev, I. V., Rezanov, I. V., Trenikhin, M. V., & Lavrenov, A. V. (2024). Influence of the structure of carbon black on its electrical conductivity and adsorption properties. *Journal of Materials Science*, *59*(37), 17517–17530. https://doi.org/10.1007/s10853-024-10245-y

Attademo, A. M., Sanchez-Hernandez, J. C., Lajmanovich, R. C., Repetti, M. R., & Peltzer, P. M. (2021). Enzyme Activities as Indicators of Soil Quality: Response to Intensive Soybean and Rice Crops. *Water, Air, and Soil Pollution*, *232*(7). https://doi.org/10.1007/s11270-021-05211-2

Birol, M., & Günal, H. (2025). Long-Term Effects of Biochar Amendments on Soil Moisture Dynamics and Selected Physical Properties in Clayey Soil of Bafra plain, Turkiye. *Communications in Soil Science and Plant Analysis*, *56*(16), 2429–2442. https://doi.org/10.1080/00103624.2025.2513632

Blake, G. R. (2015). Bulk density. In *Methods of Soil Analysis, Part 1: Physical and Mineralogical Properties, Including Statistics of Measurement and Sampling* (pp. 374–390). wiley. https://doi.org/10.2134/agronmonogr9.1.c30

Blake, G. R., & Hartge, K. H. (2018). Particle density. In *Methods of Soil Analysis, Part 1: Physical and Mineralogical Methods* (pp. 377–382). wiley. https://doi.org/10.2136/sssabookser5.1.2ed.c14

Blanco-Canqui, H. (2017). Biochar and Soil Physical Properties. *Soil Science Society of America Journal*, *81*(4), 687–711. https://doi.org/10.2136/sssaj2017.01.0017

Braga, R. M., Melo, D. M. A., Melo, M. A. F., Freitas, J. C. O., & Boateng, A. A. (2022). Effect of pretreatment on pyrolysis products of Pennisetum purpureum Schum. by Py-GC/MS. *Journal of Thermal Analysis and Calorimetry*, *147*(12), 6655–6663. https://doi.org/10.1007/s10973-021-11025-5

Chapman, H. D. (2016). Cation-exchange capacity. In *Methods of Soil Analysis, Part 2: Chemical and Microbiological Properties* (pp. 891–901). wiley. https://doi.org/10.2134/agronmonogr9.2.c6

Chen, M., Masum, S., & Thomas, H. (2021). Modeling Adsorption and Transport behavior of Gases in Moist Coal Matrix. *Energy and Fuels*, *35*(16), 13200–13214. https://doi.org/10.1021/acs.energyfuels.1c01334

Chowdhury, Z. Z., Ziaul Karim, M., Ashraf, M. A., & Khalid, K. (2016). Influence of carbonization temperature on physicochemical properties of biochar derived from slow pyrolysis of durian wood (Durio zibethinus) sawdust. *BioResources*, *11*(2), 3356–3372. https://doi.org/10.15376/biores.11.2.3356-3372

Chrysargyris, A., & Xylia, P. (2021). Effect of the nutrient solution electrical conductivity (EC) on the growth, development and nutrient content of Viola tricolor var. Hortensis grown in perlite. *Acta Horticulturae*, *1321*, 149–156. https://doi.org/10.17660/ActaHortic.2021.1321.19

Ćirić, V., Prekop, N., Šeremešić, S., Vojnov, B., Pejić, B., Radovanović, D., & Marinković, D. (2023). THE IMPLICATION OF CATION EXCHANGE CAPACITY (CEC) ASSESSMENT FOR SOIL QUALITY MANAGEMENT AND IMPROVEMENT. *Agriculture and Forestry*, *69*(4), 113–134. https://doi.org/10.17707/AgricultForest.69.4.08

Cui, D., Chang, H., Zhang, X., Pan, S., & Wang, Q. (2020). Pyrolysis temperature effect on compositions of neutral nitrogen and acidic species in shale oil using negative-Ion ESI FT-ICR MS. *ACS Omega*, *5*(37), 23940–23950. https://doi.org/10.1021/acsomega.0c03198

Das, S. K., & Ghosh, G. K. (2022). Hydrogel-biochar composite for agricultural applications and controlled release fertilizer: A step towards pollution free environment. *Energy*, *242*.

https://doi.org/10.1016/j.energy.2021.122977

Dhar, S. A., Sakib, T. U., & Hilary, L. N. (2022). Effects of pyrolysis temperature on production and physicochemical characterization of biochar derived from coconut fiber biomass through slow pyrolysis process. *Biomass Conversion and Biorefinery*, *12*(7), 2631–2647. https://doi.org/10.1007/s13399-020-01116-y

dos Santos, W. M., Gonzaga, M. I. S., da Silva, J. A., de Almeida, A. Q., de Jesus Santos, J. C., Gonzaga, T. A. S., da Silva Lima, I., & Araújo, E. M. (2021). Effectiveness of different biochars in remediating a salt-affected Luvisol in Northeast Brazil. *Biochar*, *3*(2), 149–159. https://doi.org/10.1007/s42773-020-00084-w

E., B., & V., M. (2023). Improving physical properties of sandy soil by Si-Rich amendments. In *Advantages and Disadvantages of Sandy Soils*. https://www.scopus.com/pages/publications/85147909615?origin=scopusAI

Egamberdieva, D., Alaylar, B., Kistaubayeva, A., Wirth, S., & Bellingrath-Kimura, S. D. (2022). Biochar for Improving Soil Biological Properties and Mitigating Salt Stress in Plants on Salt-affected Soils. *Communications in Soil Science and Plant Analysis*, *53*(2), 140–152. https://doi.org/10.1080/00103624.2021.1993884

Fahmi, A., Nurzakiah, S., & Susilawati, A. (2019). The interaction of peat and sulphidic material as substratum in wetland: Ash content and electrical conductivity dynamic. *IOP Conference Series: Earth and Environmental Science*, *393*(1). https://doi.org/10.1088/1755-1315/393/1/012045

Fang, C., Wu, H., Lee, S. Y., Mahajan, R. L., & Qiao, R. (2018). The ionized graphene oxide membranes for water-ethanol separation. *Carbon*, *136*, 262–269. https://doi.org/10.1016/j.carbon.2018.04.077

Fatimah, S., Ragadhita, R., Al Husaeni, D. F., & Nandiyanto, A. B. D. (2022). How to Calculate Crystallite Size from X-Ray Diffraction (XRD) using Scherrer Method. *ASEAN Journal of Science and Engineering*, *2*(1), 65–76. https://doi.org/10.17509/ajse.v2i1.37647

Fernandes, B. C. C., Mendes, K. F., Júnior, A. F. D., Caldeira, V. P. da S., Teófilo, T. M. da S., Silva, T. S., Mendonça, V., de Freitas Souza, M., & Silva, D. V. (2020). Impact of pyrolysis temperature on the properties of eucalyptus wood-derived biochar. *Materials*, *13*(24), 1–13. https://doi.org/10.3390/ma13245841

Fidel, R. B., Laird, D. A., & Spokas, K. A. (2018). Sorption of ammonium and nitrate to biochars is electrostatic and pH-dependent. *Scientific Reports*, *8*(1). https://doi.org/10.1038/s41598-018-35534-w

Flint, L. E., & Flint, A. L. (2018). Porosity. In *Methods of Soil Analysis, Part 4: Physical Methods* (pp. 241–254). wiley. https://doi.org/10.2136/sssabookser5.4.c11

Gee, G. W., & Or, D. (2018). Particle-Size Analysis. In *Methods of Soil Analysis, Part 4: Physical Methods* (pp. 255–293). wiley. https://doi.org/10.2136/sssabookser5.4.c12

Greinert, A., Mrówczynska, M., & Szefner, W. (2019). Study on the possibilities of natural use of ash granulate obtained from the combustion of pellets from plant biomass. *Energies*, *12*(13). https://doi.org/10.3390/en12132569

Helepciuc Gradinaru, C. M., Barbuta, M., Ciocan, V., Serbanoiu, A. A., & Gradinaru, A. C. (2017). Health and environmental effects of heavy metals resulted from fly ash and cement obtaining and trials to reduce their pollutant concentration by a process of combining-exclusion. *International Multidisciplinary Scientific GeoConference Surveying Geology and Mining Ecology Management, SGEM*, *17*(52), 441–447. https://doi.org/10.5593/sgem2017/52/S20.057

Huang, Y., Li, F., Meng, J., & Chen, W. (2019). Lignin content of agro-forestry biomass negatively affects the resultant biochar pH. *BioResources*, *13*(3), 5153–5163. https://doi.org/10.15376/biores.13.3.5153-5163

Jiang, Y., Tian, Y., & Qiao, Y. (2021). Analysis of Pressurized Pyrolysis Behavior of Yichun Coal at Different Temperature with Gas Chromatography and Mass Spectrometer. *Journal of Physics: Conference Series*, *2083*(2). https://doi.org/10.1088/1742-6596/2083/2/022008

John, J., Hugar, K. M., Rivera-Meléndez, J., Kostalik, H. A., Rus, E. D., Wang, H., Coates, G. W., & Abruña, H. D. (2014). An electrochemical quartz crystal microbalance study of a prospective alkaline anion exchange membrane material for fuel cells: Anion exchange dynamics and membrane swelling.

Journal of the American Chemical Society, *136*(14), 5309–5322. https://doi.org/10.1021/ja4117457

Lan, Y., Meng, J., Han, X. R., & Chen, W. F. (2024). Advances in research on biochar-based products and their effects on soil fertility improvement[生物炭基产品及其对土壤培肥改良效应的研究进展]. *Journal of Plant Nutrition and Fertilizers*, *30*(7), 1396–1412. https://doi.org/10.11674/zwyf.2024276

Li, C., Ahmed, W., Li, D., Yu, L., Xu, L., Xu, T., & Zhao, Z. (2022). Biochar suppresses bacterial wilt disease of flue-cured tobacco by improving soil health and functional diversity of rhizosphere microorganisms. *Applied Soil Ecology*, *171*. https://doi.org/10.1016/j.apsoil.2021.104314

Li, X., Wang, X., Zhao, Q., Zhang, Y., & Zhou, Q. (2016). In situ representation of soil/sediment conductivity using electrochemical impedance spectroscopy. *Sensors (Switzerland)*, *16*(5). https://doi.org/10.3390/s16050625

Li, Y., Sang, Z., Zhao, Z., Zhu, L., Shi, X., Lu, H., Yingli, S., Ke, P., & Zhang, G. (2025). The Effect of Calibration with Different Matrix Reference Materials on the Accuracy of Oxygen Determination by Inert Gas Fusion-Infrared Absorptiometry. *Journal of Physics: Conference Series*, *2959*(1). https://doi.org/10.1088/1742-6596/2959/1/012004

Li, Y., Yang, W., Wang, W., Yu, N., Liu, P., Zhao, B., Zhang, J., & Ren, B. (2025). Dual film-controlled model urea improves summer maize yields, N fertilizer use efficiency and reduces greenhouse gas emissions. *Soil and Tillage Research*, *252*. https://doi.org/10.1016/j.still.2025.106565

Lin, Y., Yan, W., & Sheng, K. (2016). Effect of pyrolysis conditions on the characteristics of biochar produced from a tobacco stem. *Waste Management and Research*, *34*(8), 793–801. https://doi.org/10.1177/0734242X16654977

Liu, X., Liao, J., Song, H., Yang, Y., Guan, C., & Zhang, Z. (2019). A Biochar-Based Route for Environmentally Friendly Controlled Release of Nitrogen: Urea-Loaded Biochar and Bentonite Composite. *Scientific Reports*, *9*(1). https://doi.org/10.1038/s41598-019-46065-3

Melo, L. C. A., Lehmann, J., Carneiro, J. S. da S., & Camps-Arbestain, M. (2022). Biochar-based fertilizer effects on crop productivity: a meta-analysis. In *Plant and Soil* (Vol. 472, Issues 1–2, pp. 45–58). Springer Science and Business Media Deutschland GmbH. https://doi.org/10.1007/s11104-021-05276-2

Mohan, M., Banerjee, T., & Goud, V. V. (2015). Hydrolysis of bamboo biomass by subcritical water treatment. *Bioresource Technology*, *191*(May), 244–252. https://doi.org/10.1016/j.biortech.2015.05.010

Mohd Fairulnizal, M. N., Vimala, B., Rathi, D. N., & Mohd Naeem, M. N. (2019). Atomic absorption spectroscopy for food quality evaluation. In *Evaluation Technologies for Food Quality* (pp. 145–173). Elsevier. https://doi.org/10.1016/B978-0-12-814217-2.00009-3

Mulyatini, N., Herlina, E., Akbar, D. S., & Eko Prabowo, F. H. (2023). Analisis potensi pembentukan kawasan industri hasil tembakau dalam perspektif ekonomi. *JPPI (Jurnal Penelitian Pendidikan Indonesia)*, *9*(1), 334. https://doi.org/10.29210/020231920

Nan, Z., Floquet, P., Combes, D., Tendero, C., & Castelain, M. (2023). Surface Conditioning Effects on Submerged Optical Sensors: A Comparative Study of Fused Silica, Titanium Dioxide, Aluminum Oxide, and Parylene C. *Sensors*, *23*(23). https://doi.org/10.3390/s23239546

Oktariani, P., Hidayat, M., Tjahyandari, D., & Suwardi. (2023). Comparison of horticultural crop growth planted on zeoponic and commercial growth media. *AIP Conference Proceedings*, *2732*. https://doi.org/10.1063/5.0133369

Palupi, B., Aji, B. B., Prasiefa, M. G., Putri, D. K. Y., Rahmawati, I., Fachri, B. A., Rizkiana, M. F., & Amini, H. W. (2023). Microwave-Assisted Hydrolysis Batang Tembakau untuk Produksi Gula Pereduksi sebagai Bahan Baku Bioetanol. *Jurnal Teknologi*, *10*(2). https://doi.org/10.31479/JTEK.V10I2.225

Polat, S., Apaydin-Varol, E., & Pütün, A. E. (2016). Thermal decomposition behavior of tobacco stem Part I: TGA–FTIR–MS analysis. *Energy Sources, Part A: Recovery, Utilization and Environmental Effects*, *38*(20), 3065–3072. https://doi.org/10.1080/15567036.2015.1129373

Prasiefa, M. G., & Zullaikah, S. (2025). Effect of Different Operating Conditions on Tobacco Stem Pyrolysis and Impregnation for Further Controlled Release Fertiliser Application. *Materials Science Forum*, *1154*, 79–84. https://doi.org/10.4028/P-2BYN6B

Qurat-ul-Ain, Shafiq, M., Capareda, S. C., & Firdaus-e-Bareen. (2021). Effect of different temperatures on

the properties of pyrolysis products of Parthenium hysterophorus. *Journal of Saudi Chemical Society*, *25*(3). https://doi.org/10.1016/j.jscs.2021.101197

Racero-Galaraga, D., Rhenals-Julio, J. D., Sofan-German, S., Mendoza, J. M., & Bula-Silvera, A. (2024). Proximate analysis in biomass: Standards, applications and key characteristics. *Results in Chemistry*, *12*. https://doi.org/10.1016/j.rechem.2024.101886

Rahmat, A., Zahrani, A., Hidayat, H., Arum, F., Respati, S. A., Susanti, W. D., Hariadi, H., & Mutolib, A. (2025). Characteristics of Jengkol Peel (Pithecellobium jiringa) Biochar Produced at Various Pyrolysis Temperatures for Enhanced Agricultural Waste Management and Supporting Sustainable Development Goals (SDGs). *ASEAN Journal of Science and Engineering*, *5*(1), 145–172. https://doi.org/10.17509/ajse.v5i1.81297

Ramesh, K., Dinakarkumar, Y., Gujjula, K. R., Kotaru, L. S., Brindha Devi, P., Pazhamalai, V., & Ivo Romauld, S. (2025). Impacts of Biomass-Derived Biochar on Plant Nutrition, Soil Function, and Agricultural Sustainability: A Review. *Environmental Quality Management*, *35*(2). https://doi.org/10.1002/tqem.70198

Ramontja, J., Iwuozor, K. O., Emenike, E. C., Okorie, C. J., Saka, H. B., Ezzat, A. O., Adeleke, J. A., Saliu, O. D., & Adeniyi, A. G. (2025). From tobacco to biochar: a review of production processes, properties, and applications. *Biofuels, Bioproducts and Biorefining*, *19*(3), 911–928. https://doi.org/10.1002/bbb.2728

Schulz, B., Sandmann, D., & Gilbricht, S. (2020). Sem-based automated mineralogy and its application in geo-and material sciences. *Minerals*, *10*(11), 1–26. https://doi.org/10.3390/min10111004

Shahid, M., Srivastava, S., Shukla, P., Yadav, R., Sajid, M., Kumar, A., Singh, S., & Bharadwaj, M. (2023). Characterization of physiochemical parameters & their effect on microbial content of smokeless tobacco products marketed in north India. *Indian Journal of Medical Research*, *158*(56), 542–551. https://doi.org/10.4103/ijmr.ijmr_1467_22

Shi, R. Y., Hong, Z. N., Li, J. Y., Jiang, J., Baquy, M. A. Al, Xu, R. K., & Qian, W. (2017). Mechanisms for Increasing the pH Buffering Capacity of an Acidic Ultisol by Crop Residue-Derived Biochars. *Journal of Agricultural and Food Chemistry*, *65*(37), 8111–8119. https://doi.org/10.1021/acs.jafc.7b02266

Shin, S. G. (2015). Dependency of the critical carbon content of electrical conductivity for carbon powder-filled polymer matrix composites. *Korean Journal of Materials Research*, *25*(8), 365–369. https://doi.org/10.3740/MRSK.2015.25.8.365

Siewruk, K., & Szulc, W. (2023). Assessment of the effect of intensive agricultural production on nutrient movement in soil[Ocena wpływu intensywnej produkcji rolnej na przemieszczanie się składników pokarmowych w glebie]. *Soil Science Annual*, *74*(3). https://doi.org/10.37501/soilsa/171629

Simmons, C. A. (2017). Biochar: Chemical composition, soil applications and ecological impacts. In *Biochar: Chemical Composition, Soil Applications and Ecological Impacts*. https://www.scopus.com/pages/publications/85035088424?origin=scopusAI

Sorrenti, G., Masiello, C. A., Dugan, B., & Toselli, M. (2016). Biochar physico-chemical properties as affected by environmental exposure. *Science of the Total Environment*, *563–564*, 237–246. https://doi.org/10.1016/j.scitotenv.2016.03.245

Sukamto, Samanhudi, D., Sunardi, & Siswati, N. D. (2016). Pyrolisator coal to be cokes (coal cokes) casting metal industry standard. *MATEC Web of Conferences*, *58*. https://doi.org/10.1051/matecconf/20165801015

Suwardi, Palupiningtyas, E., Nur Fatiha, Y. G., Hidayat, M., Suryaningtyas, D. T., & Oktariani, P. (2023). Chemical and physical properties of zeoponic and their influence on growth of forestry plant seedling and horticultural crops. *IOP Conference Series: Earth and Environmental Science*, *1133*(1). https://doi.org/10.1088/1755-1315/1133/1/012019

Vyavahare, G. D., Lee, Y., Seok, Y. J., Kim, H. N., Sung, J., & Park, J. H. (2023). Monitoring of Soil Nutrient Levels by an EC Sensor during Spring Onion (Allium fistulosum) Cultivation under Different Fertilizer Treatments. *Agronomy*, *13*(8). https://doi.org/10.3390/agronomy13082156

Wang, C., Li, L., Chen, R., Ma, X., Lu, M., Ma, W., & Peng, H. (2019). Thermal conversion of tobacco stem into gaseous products. *Journal of Thermal Analysis and Calorimetry*, *137*(3), 811–823. https://doi.org/10.1007/s10973-019-08010-4

Wang, D., Li, C., Parikh, S. J., & Scow, K. M. (2019). Impact of biochar on water retention of two agricultural soils – A multi-scale analysis. *Geoderma*, *340*, 185–191. https://doi.org/10.1016/j.geoderma.2019.01.012

Wang, H., Luo, F., Li, Y., Li, D., Zhao, R., & Li, F. (2018). Emission analysis from thermal decomposition of different tobacco materials by thermogravimetric analysis coupled cold trap and GC/MS[热重-冷阱捕集-气相色谱/质谱法分析不同烟草基质受热过程中的逸出物]. *Tobacco Science and Technology*, *51*(1), 50–58. https://doi.org/10.16135/j.issn1002-0861.2017.0099

Wang, Y., Chen, Z., & Hu, L. (2023). Determining the Geometric Surface Area of Mesoporous Materials. *Journal of Physical Chemistry C*, *127*(9), 4799–4807. https://doi.org/10.1021/acs.jpcc.3c00162

Wang, Y. Y., Wang, Y. M., Gao, X. H., Deng, S. W., & Li, S. (2020). Review on the application of X-ray fluorescence spectrometry in rock analysis[X射线荧光光谱在岩石分析中的应用评介]. *Yejin Fenxi/Metallurgical Analysis*, *40*(10), 1–11. https://doi.org/10.13228/j.boyuan.issn1000-7571.011079

Wardman, J. B., Wilson, T. M., Bodger, P. S., Cole, J. W., & Johnston, D. M. (2012). Investigating the electrical conductivity of volcanic ash and its effect on HV power systems. *Physics and Chemistry of the Earth*, *45–46*, 128–145. https://doi.org/10.1016/j.pce.2011.09.003

Weber, K., & Quicker, P. (2018). Properties of biochar. In *Fuel* (Vol. 217, pp. 240–261). Elsevier Ltd. https://doi.org/10.1016/j.fuel.2017.12.054

Wei, B., Peng, Y., Lin, L., Zhang, D., Ma, L., Jiang, L., Li, Y., He, T., & Wang, Z. (2023). Drivers of biochar-mediated improvement of soil water retention capacity based on soil texture: A meta-analysis. *Geoderma*, *437*. https://doi.org/10.1016/j.geoderma.2023.116591

Weisenberger, T. B., Ingimarsson, H., Hersir, G. P., & Flóvenz, Ó. G. (2020). Cation-exchange capacity distribution within hydrothermal systems and its relation to the alteration mineralogy and electrical resistivity. *Energies*, *13*(21). https://doi.org/10.3390/en13215730

Wu, Q., Qiao, Y., Zhou, Q., Chen, J., & Wang, G. (2023). Controlled-Release Blended Fertilizer Combined with Urea Reduces Nitrogen Losses by Runoff and Improves Nitrogen Use Efficiency and Yield of Wet Direct-Seeded Rice in Central China. *Sustainability (Switzerland)*, *15*(16). https://doi.org/10.3390/su151612336

Wu, X. F., Li, S. X., & Li, M. F. (2019). Effect of temperature on the properties of charcoal prepared from carbonization of biorefinery lignin. *BioResources*, *13*(3), 6736–6745. https://doi.org/10.15376/biores.13.3.6736-6745

X.A., L., A.H., P., Q.V., N., T.H., T., T.T.T., N., & author, +1. (2020). Research and produce fertilizer from npk fertilizer and biochar for agricultural production. *ARPN Journal of Engineering and Applied Sciences*. https://www.scopus.com/pages/publications/85080134255?origin=scopusAI

Xu, Z., Zhou, R., & Xu, G. (2025). Global analysis on potential effects of biochar on crop yields and soil quality. *Soil Ecology Letters*, *7*(1). https://doi.org/10.1007/s42832-024-0267-x

Xue, S., Zhu, F., Kong, X., Wu, C., Huang, L., Huang, N., & Hartley, W. (2016). A review of the characterization and revegetation of bauxite residues (Red mud). *Environmental Science and Pollution Research*, *23*(2), 1120–1132. https://doi.org/10.1007/s11356-015-4558-8

Yang, M., Zhou, D., Hang, H., Chen, S., Liu, H., Su, J., Lv, H., Jia, H., & Zhao, G. (2024). Effects of Balancing Exchangeable Cations Ca, Mg, and K on the Growth of Tomato Seedlings (Solanum lycopersicum L.) Based on Increased Soil Cation Exchange Capacity. *Agronomy*, *14*(3). https://doi.org/10.3390/agronomy14030629

Yang, T., Yu, L., Tong, Y., Kai, X., Zhai, Y., Li, B., & Li, R. (2023). Influence of original and additive AAEMs on the migration and transformation of N by pyrolysis in Fushun oil shale. *Journal of Analytical and Applied Pyrolysis*, *171*. https://doi.org/10.1016/j.jaap.2023.105970

Yang, X., Yang, M., An, H., Chen, H., Zhang, S., & Liang, Z. (2018). Analysis on pyrolysis process and physicochemical properties of char fuels deprived from corn cobs[玉米芯炭质燃料的理化性能及热解过程分析]. *Guocheng Gongcheng Xuebao/The Chinese Journal of Process Engineering*, *18*(4), 851–857. https://doi.org/10.12034/j.issn.1009-606X.217376

Yashim, M. M., Razali, N., Saadon, N., & Rahman, N. A. (2016). Effect of activation temperature on properties of activated carbon prepared from oil palm kernel shell (OPKS). *ARPN Journal of Engineering*

and Applied Sciences. https://www.scopus.com/pages/publications/84971457404?origin=scopusAI

Yi, L., Feng, J., Qin, Y. H., & Li, W. Y. (2017). Prediction of elemental composition of coal using proximate analysis. *Fuel*, *193*, 315–321. https://doi.org/10.1016/j.fuel.2016.12.044

Zarzuela, R., Domínguez, M., Carbú, M., Moreno-Garrido, I., Diaz, A., Cantoral, J. M., Gil, M. L. A., & Mosquera, M. J. (2023). Studying the influence of surface properties on the cell attachment and anti-fouling capacity of Ag/SiO2 superhydrophobic coatings for building materials. *Building and Environment*, *243*. https://doi.org/10.1016/j.buildenv.2023.110707

Zhao, S. X., Ta, N., & Wang, X. D. (2017). Effect of temperature on the structural and physicochemical properties of biochar with apple tree branches as feedstock material. *Energies*, *10*(9). https://doi.org/10.3390/en10091293

Zhao, Z. Z., Wang, X. L., Li, H. B., Ren, S. P., Chen, J., & Wang, L. L. (2021). Slow-release property and soil remediation mechanism of biochar-based fertilizers. *Journal of Plant Nutrition and Fertilizers*, *27*(5), 886–897. https://doi.org/10.11674/zwyf.20472

Zheng, K., Zhang, S. Q., Liu, H. F., Zhang, X. Q., & Huang, Y. (2019). Effect of Different Treatments on Sr(Ⅱ) Adsorption on Biochar[不同处理方式对生物炭吸附Sr(Ⅱ)的影响机制]. *He-Huaxue Yu Fangshe Huaxue/Journal of Nuclear and Radiochemistry*, *41*(5), 492–502. https://doi.org/10.7538/hhx.2019.YX.2019037

Zhu, Y., Tan, Z., Liu, H., Zhang, W., Huo, G., Yang, W., Lv, L., Yang, H., & Lei, T. (2023). Effects of volatile-char interaction on the product properties from municipal sludge pyrolysis. *Fuel*, *335*. https://doi.org/10.1016/j.fuel.2022.126936

Zulkifli, N. N. I., Abdullah, M. M. A. B., Przybył, A., Pietrusiewicz, P., Salleh, M. A. A. M., Aziz, I. H., Kwiatkowski, D., Gacek, M., Gucwa, M., & Chaiprapa, J. (2021). Influence of sintering temperature of kaolin, slag, and fly ash geopolymers on the microstructure, phase analysis, and electrical conductivity. *Materials*, *14*(9). https://doi.org/10.3390/ma14092213